STUDY OF CALCIUM PHOSPHATE (DCPD) ELECTRODEPOSITION PROCESS ON THE Mg-3Al-1Zn MAGNESIUM ALLOY SURFACE

Filip Pastorek[1,*], Branislav Hadzima[1]

[1]Department of Materials Engineering, Faculty of Mechanical Engineering, University of Žilina, Univerzitná 1, 010 26 Žilina, Slovak republic
[*]Corresponding author e-mail: filip.pastorek@fstroj.uniza.sk

Resume
Evaluation of calcium phosphating process realized on the Mg-3Al-1Zn alloy surface after grinding was investigated by electrochemical tests supported by photodocumentation. The electrodeposition treatment was performed by electrochemical method in water solution of $Ca(NO_3)_2.4H_2O$, $(NH_4)_2HPO_4$ and H_2O_2. The formation of calcium phosphate was divided into several stages and described using light microscopy. The progress in corrosion protection of created calcium phosphate layer in 0.9% NaCl after particular electrodeposition steps was evaluated by electrochemical impedance spectroscopy. The results in the form of Nyquist plots were analyzed using equivalent circuits.

Available online: http://fstroj.uniza.sk/journal-mi/PDF/2013/07-2013.pdf

Article info

Article history:
Received 20 September 2012
Accepted 2 November 2012
Online 24 February 2013

Keywords:
Calcium phosphate;
Magnesium alloy;
Electrochemical impedance spectroscopy;
Light microscopy;
Electrodeposition

ISSN 1335-0803 (print version)
ISSN 1338-6174

1. Introduction

Biodegradable implant materials are being developed to achieve complete dissolution of the implant after healing without the need for any additional surgeries to remove it [1, 2]. Further, the use of these biodegradable implants eliminates the complications associated with the long-term application of such devices in the human body. Polymeric materials, such as polyglycolic acid (PGA), polylactic acid (PLA), and polydioxanone (PDS) were used as commercial biodegradable and bioabsorbable implants [3, 4]. However, these materials are limited by their low mechanical properties and radiolucency [5]. Metals have desirable mechanical properties due to their relatively high strength and fracture toughness; however, the majority of metals are either biologically nonabsorbable or toxic. Studies have shown that the most commonly used materials for implants, viz., stainless steel-, cobalt-, chromium-, and nickel-based alloys produce corrosion products that are harmful to the human body [6–10].

Magnesium has been suggested as a revolutionary implant material to overcome the limitations of the current metallic materials being used. Mg is light in weight and low in density, and exhibits high strength/weight ratio [11]. The elastic modulus of Mg has been reported as 45 GPa [7] and therefore, in comparison with the current metals in clinical use, is far closer to the elastic modulus of bone. Mg also has the advantage of degradation, and thus if corrosion rates are controlled, the material would slowly degrade, removing the necessity for second removal surgeries, thereby decreasing health risks, costs and scarring. Additionally, in contrast to the metals currently utilized, the wear products of which can be potentially toxic or otherwise harmful to the patient [12–15], the corrosion products of Mg

have been shown to be potentially beneficial to the patient [16].

The degradable properties of Mg and its alloys are, however, a double-edged sword. Mg is a highly reactive metal, and corrosion rates when immersed in physiological solutions are high. In order for use of this material to be feasible for orthopedic applications, the corrosion mechanisms must be reduced and controlled. In response to this, coatings have been suggested as a means of reducing exposure to the corrosive environment, thus reducing the corrosion rate. Ideally, corrosion would be slowed to allow the mechanical integrity of the metal to remain intact during bone healing. This would also minimize hydrogen production, which has been observed as a (potentially disadvantageous) corrosion by product when using this material [17–20]. Theoretically, it would be then expected a coating to slowly wear away, allowing controlled degradation of the substrate [21]

One of the most perspective coatings for implants are calcium phosphates, including hydroxyapatite (HA), octacalcium phosphate (OCP) and brushite (DCPD - dicalcium phosphate dehydrate), because of their excellent biocompatibility, non-toxicity and bioactivity [22]. In addition, it was reported the magnesium alloy promotes or accelerates the deposition of calcium and phosphate [23, 24].

Actually, some magnesium alloys containing Zr, Cd, rare earth elements and heavy metals are not suitable for biomaterials application from the medical aspect [25, 26]. But the mechanical and corrosion properties of pure magnesium are unsatisfactory. In comparison with other magnesium alloys, AZ31 magnesium alloy, with low Al content, good mechanical properties and corrosion resistance, is suitable to act as biodegradable material [26]. Even though the biocompatibility of aluminium is limited [27], it seems to be a valid alloying element for magnesium alloys in body contact, as it is known to diminish the magnesium corrosion rate by stabilizing hydroxides in chloride environments [19, 28] The addition of Zn to Mg results in improved mechanical properties thanks to grain refinement, and shows a reduced corrosion rate compared with pure Mg [29, 30].

For these reasons, the aim of this study is to electrodeposit calcium phosphate layer on magnesium alloy AZ31 surface and to improve its corrosion properties by this way.

2. Experimental material and methods

The tested AZ31 magnesium alloy was continually casted at Brandenburgische Universität in Cottbus, Germany and chemical composition was analyzed at the Magnesium innovation centre MagIC GKSS Geesthacht, Germany. The chemical composition is listed in Table 1. The specimens for metallographic observation were prepared by conventional metallographic procedures. For visualization of the magnesium alloy microstructure, etchant consisting of 2.5 ml acetic acid + 2.1 g picric acid + 5 ml H2O + 35 ml of ethanol was used [31]. The microstructure of AZ31 alloy (Fig. 1) was observed by the CARL ZEISS AXIO Imager.A1m light metallographic microscope in the laboratories of Department of Materials Engineering, University of Žilina.

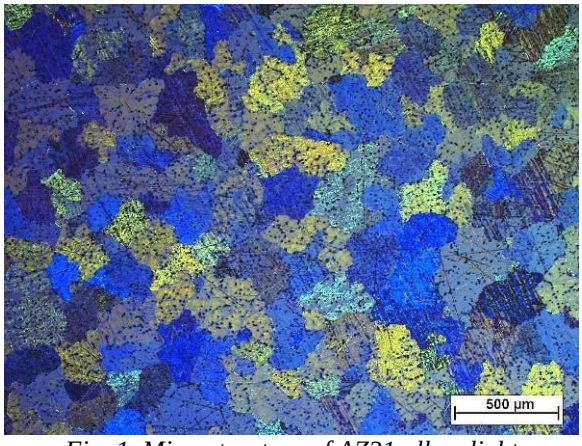

Fig. 1. Microstructure of AZ31 alloy, light microscopy (polarized light), etch. acetic acid + picric acid + water + ethanol
(full colour version available online)

The microstructure is created by polyedric grains of supersaturated solid solution of aluminium, zinc and other alloying elements in magnesium. The average grain size is 220 μm.

Table 1

Chemical composition of AZ31 alloy

Component	Al	Zn	Mn	Si	Cu	Ni	Fe	Mg
wt. %	2.96	0.828	0.433	0.004	0.004	<0.001	0.002	balance

2.1. Experimental material surface preparation

For the evaluation of calcium phosphate surface treatment influence on electrochemical characteristics the specimen surfaces were grinded with 1000 grit SiC paper to ensure the same surface roughness, then rinsed with demineralised water and ethanol, and dried using a stream of air. After described pre-treating the DCPD was deposed on the specimens' surfaces. Treatment electrolyte solution was prepared with 0.1 M Ca(NO3)2.4H2O, 0.06 M NH4HPO4, 10 ml.dm-3 of 50 vol.% H2O2. Solution pH was 4 and the electrodeposition was carried out at room temperature 22 ± 2 °C. Grinded AZ31 specimen was used as the cathode, while a platinum electrode served as the anode. Electrodeposition was performed with constant potential -100 mV vs. saturated calomel electrode (SCE) for 1 hour on a laboratory apparatus VSP (producer BioLogic SAS France). After electrodeposition specimens were immediately rinsed with demineralised water and dried using a stream of air.

2.2. Experimental methods

The surface morphology of the treated specimens was assessed in the laboratories of the Department of Materials Engineering, FME, University of Žilina, by a stereomicroscope Nikon AZ100 with a digital camera using NIS Elements software. The corrosion characteristics of the untreated and DCPD-coated AZ31 after particular electrodeposition stages were evaluated by electrochemical impedance spectroscopy using a potentiostat/galvanostat/frequency response analyser VSP from BioLogic SAS France. All the corrosion experiments were performed at 22 ± 1 °C in 0.9% NaCl. A saturated calomel electrode and a platinum electrode served as the reference and auxiliary electrodes, respectively. Treated and untreated AZ31 specimens formed the working electrode (a classical three electrode system) in such a way that only 1 cm^2 area of the working electrode surface was exposed to the electrolyte solution in corrosion cell. Measurements were performed at open circuit potential with AC voltage amplitude of 10 mV in frequency range from 100 kHz to 20 mHz. EIS measurements resulted in Nyquist plots that were further analysed by software EC-Lab V10.12 using equivalent circuits shown in Fig. 2.

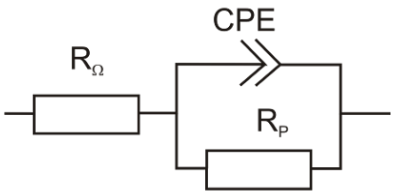

a) For Nyquist plots with one capacitive loop

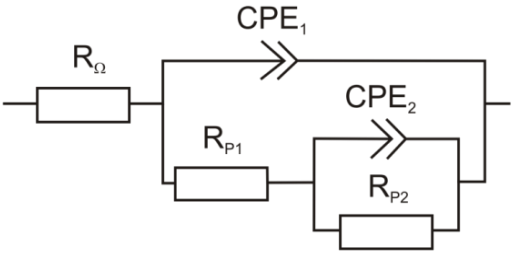

b) For Nyquist plots with two well-defined capacitive loops

Fig. 2. Equivalent circuits used for analysis of Nyquist plots

Fig. 2a express the equivalent circuit used for Nyquist plots with one capacitive loop and Fig. 2b the equivalent circuit used for Nyquist plots with two well-defined capacitive loops. These equivalent circuits use various elements expressing the character of evaluated surface. In our case, R_Ω is resistance of the solution, R_{p1} and R_{p2} are polarization resistances of various

mechanisms in corrosion model (e.g. charge transfer, film resistance, ...), R_p is mixed polarization resistance or sum of partial polarization resistances (R_{p1} + R_{p2}) and CPE_1 and CPE_2 are constant phase elements of mechanisms corresponding with R_{p1} and R_{p2}, respectively. CPE_1 in second equivalent circuit is constant phase element of the layer of corrosion products.

3. Results and discussion

Electrodeposition under specified conditions led to the creation of a thin layer of calcium phosphate (Fig. 3). As can be seen, the continuous layer covering the entire surface is composed of irregularly branched units that overlap each other. According to [10] and [32] the chemical composition of the observed layer is $CaHPO_4.2H_2O$.

Process of creation DCPD layer on the surface of magnesium alloy during electrodeposition is divided into two stages described by reactions (1) and (2) [32]:

1. stage: reduction reaction of $2H_2PO_4^-$

$$2H_2PO_4^- + 2e^- \rightarrow 2HPO_4^{2-} + H_2 \uparrow \quad (1)$$

2. stage: reaction of $2H_2PO_4^-$ with Ca^{2+}

$$Ca^{2+} + HPO_4^{2-} + 2H_2O \rightarrow CaHPO_4.2H_2O \quad (2)$$

As can be seen from the time dependence of current density in Fig. 4 recorded at VSP laboratory equipment showing behaviour of the electrodeposition process on the surface of the substrate, together with photodocumentation listed in Fig. 5, after the initial current density rise the continuous increase of current density occurs within the first 10 minutes up to its maximum value of -0.48 mA.cm^{-2}.

It is caused by heterogeneous nucleation of DCPD in certain places of the surface with the most suitable thermodynamic conditions i.e. in places where previous grinding process and technological operations led to a major increase of internal energy.

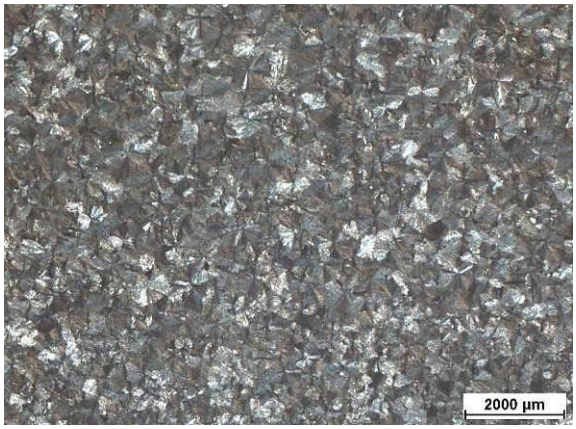

a) Overall view

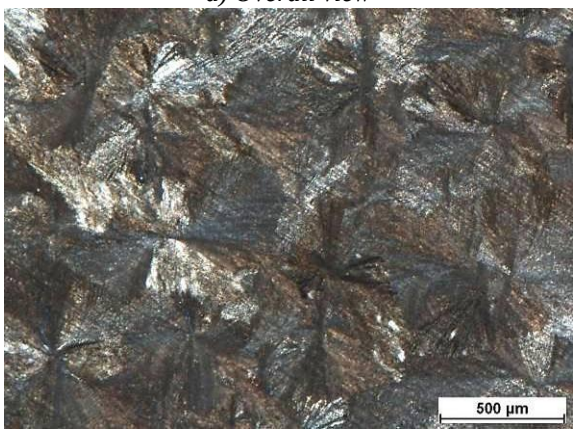

b) Detail

Fig. 3. Morphology of created calcium phosphate, light microscopy
(full colour version available online)

By increasing of electrodeposition time, increase in number of new DCPD units together with their gradual growth on the surface of the substrate is seen, that causes increment of current density about 0.044 mA.cm^{-2} per minute of electrodeposition. Once the layer-forming space branched units of DCPD cover most of the specimen surface, gradual reduction of current density (as intense as the previous growth) occurs. It is caused by the fact that increasingly smaller part of the surface participates in the intensive process of creating DCPD. Once the surface is almost completely covered with a layer of DCPD units, this leads to decrease of reduction rate of current density and its gradual fixation. This phenomenon is caused by the fact,

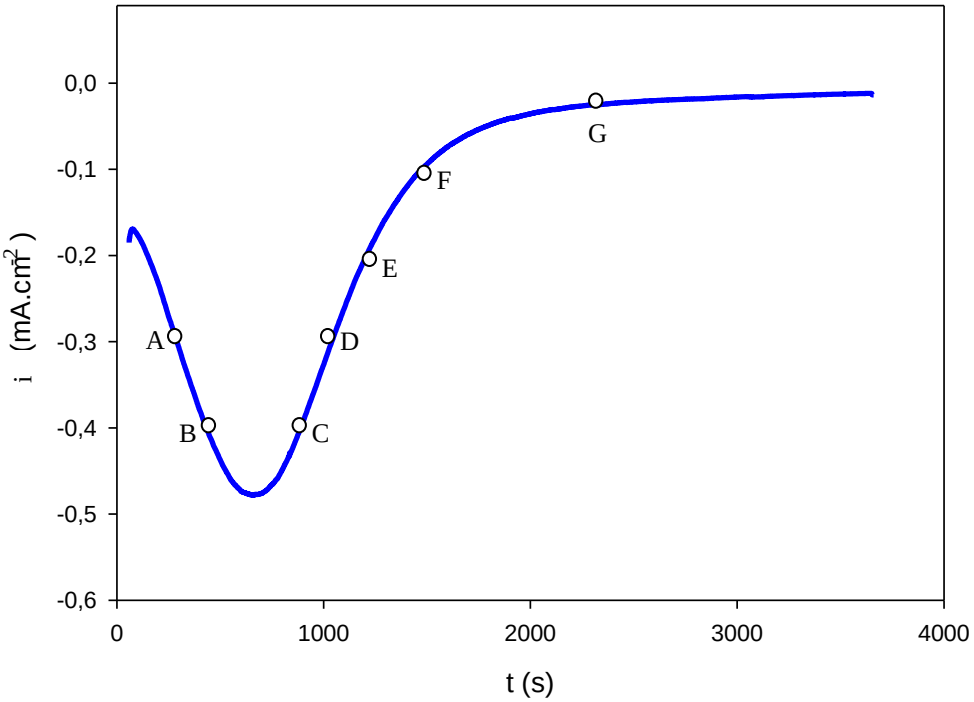

Fig. 4. Diagram of time dependence of current density during the electrodeposition process of DCPD (full colour version available online)

that nucleation of new DCPD units finishes and only gradual growth and overlapping of existing ones takes place. However, this growth and overlapping does not have such a radical impact on current density reduction rate, and thus only 0.038 $mA.cm^{-2}$ per minute current density reduction rate occurs during the second half the electrodeposition process up to its minimum value of -0.012 $mA.cm^{-2}$, what represents almost non-conducting state, that is a very significant finding in terms of electrochemical corrosion.

A very important characteristic best describing the resistance of the surface layer (or layers) of the certain material against corrosion is a polarization resistance R_p. Its values were obtained by electrochemical impedance spectroscopy, which is one the non-destructive methods for surface layers examination. By measuring R_p values after particular stages in the process of creating DCPD layer on the specimens surface (Tab. 2), an increase in the corrosion protection effect of forming DCPD during the electrodeposition process was evaluated. As can be seen from Nyquist plots measured after certain electrodeposition times (Fig. 6) respectively from the diagram representing the temporal change of polarization resistance R_p (Fig. 7), the increase of R_p is gradual, but it is possible to observe areas where this growth is more intensive. One of these areas is the electrodeposition interval between the maximum of reached current density (-0.48 $mA.cm^{-2}$, Fig. 5) and D point, where intense current density reduction appears. The second area is the last stage of the electrodeposition process (behind G point), where is although not observed a significant covering the surface by new DCPD units, but their growth and overlapping together with ultimately widening the thickness of the formed layer occurs, all resulting in a stronger increase of R_p. This gives an answer to the question why it is necessary to abide the specified electrodeposition time 1 hour, although after half an hour, not such significant decrease of the current density appears. It can be clearly stated that electrodeposition of DCPD on AZ31 specimens provides a substantial increase of R_p value compared with the value measured on pure specimens' surface after grinding. After 5 minutes of exposure in 0.9% NaCl, the R_p value of created calcium phosphate (60.627 $\Omega.cm^2$) is 43 times higher than that of just grinded surface after the same exposure time.

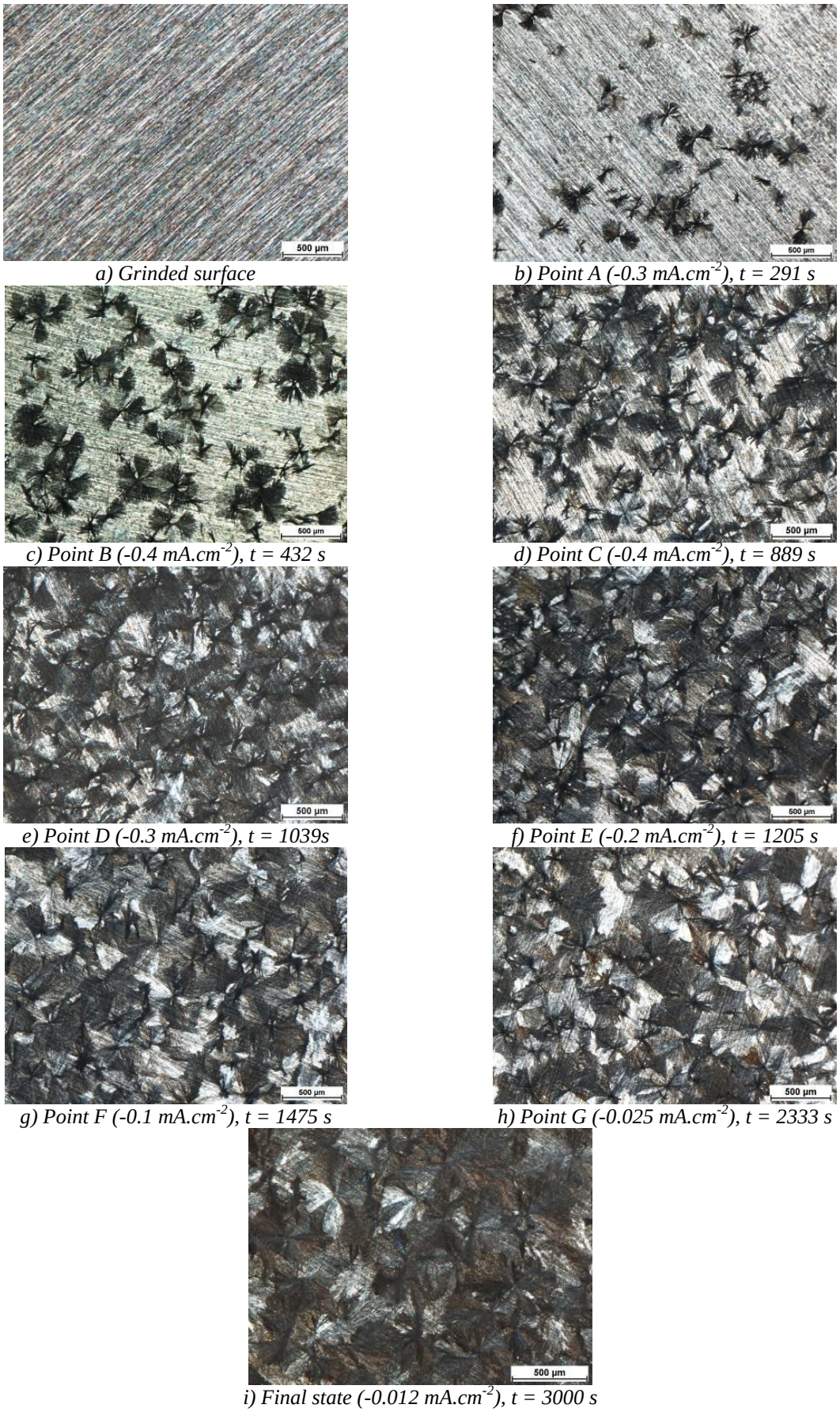

a) Grinded surface

b) Point A (-0.3 mA.cm^{-2}), t = 291 s

c) Point B (-0.4 mA.cm^{-2}), t = 432 s

d) Point C (-0.4 mA.cm^{-2}), t = 889 s

e) Point D (-0.3 mA.cm^{-2}), t = 1039s

f) Point E (-0.2 mA.cm^{-2}), t = 1205 s

g) Point F (-0.1 mA.cm^{-2}), t = 1475 s

h) Point G (-0.025 mA.cm^{-2}), t = 2333 s

i) Final state (-0.012 mA.cm^{-2}), t = 3000 s

Fig. 5. Photodocumentation of calcium phosphate creation process by electrodeposition, light microscopy
(full colour version available online)

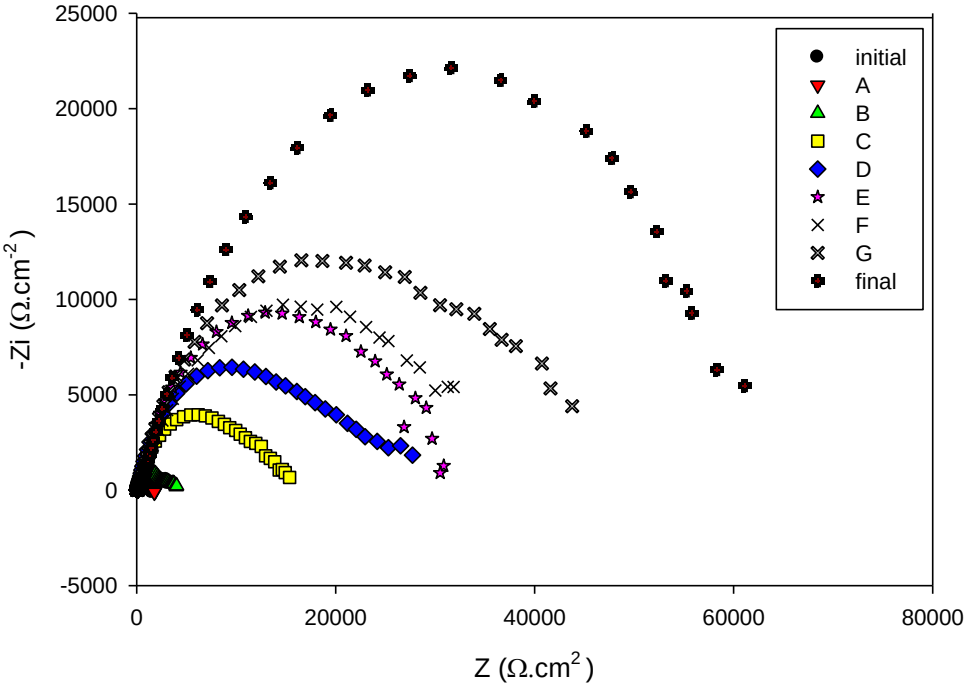

a) Complex view

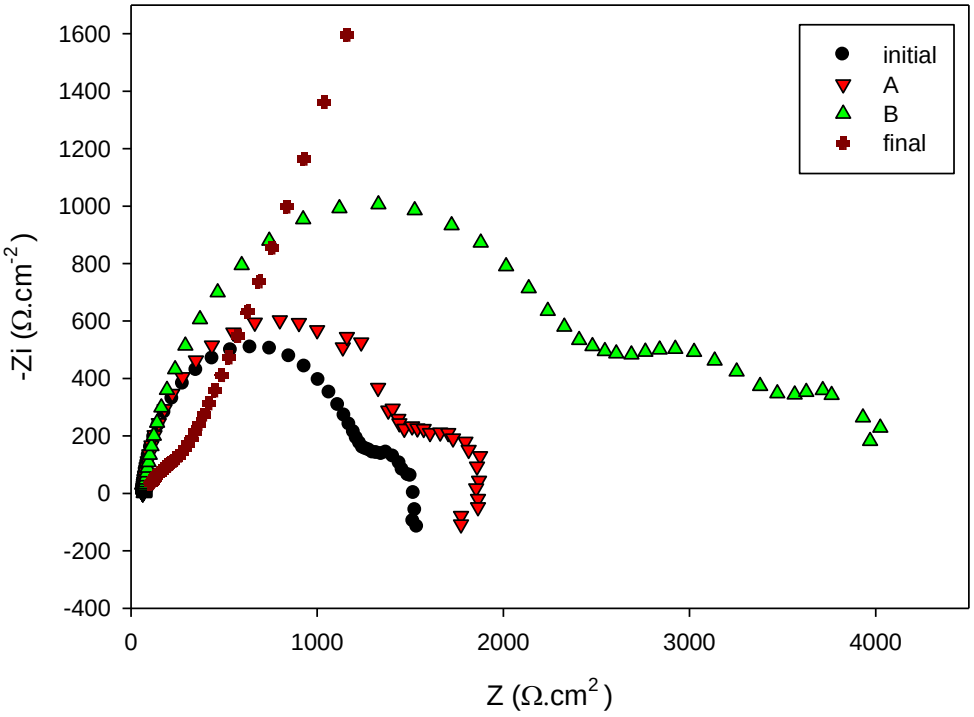

b) Detail

Fig. 6. Nyquist plots of formed surface layer on AZ31 alloy at different stages of DCPD electrodeposition (0.9% NaCl electrolyte)

(full colour version available online)

Table 2

Electrochemical characteristics of formed surface layer on AZ31 alloy surface at different stages of DCPD electrodeposition (0.9% NaCl electrolyte)

	R_Ω ($\Omega.cm^2$)	R_{p1} ($\Omega.cm^2$)	R_{p2} ($\Omega.cm^2$)	R_p ($\Omega.cm^2$)	CPE_1 ($10^{-6}.F.s^{n_1-1}$)	CPE_2 ($10^{-6}.F.s^{n_2-1}$)	n_1	n_2
Initial state	65	1157	246	1403	11	1430	0.920	1
Point A	63	1413	363	1776	13	1188	0.895	1
Point B	70	2391	1506	3897	9	603	0.895	0.733
Point C	70	11221	3790	15011	44	20	0.618	0.921
Point D	66	18747	8989	27736	58	11	0.686	0.995
Point E	73	30301	65	30366	10	1	0.743	1
Point F	62	33279	234	33513	12	55	0.706	0.469
Point G	68	40831	192	41023	9	14	0.728	0.765
Final state	60	-	-	60627	9	-	0.786	-

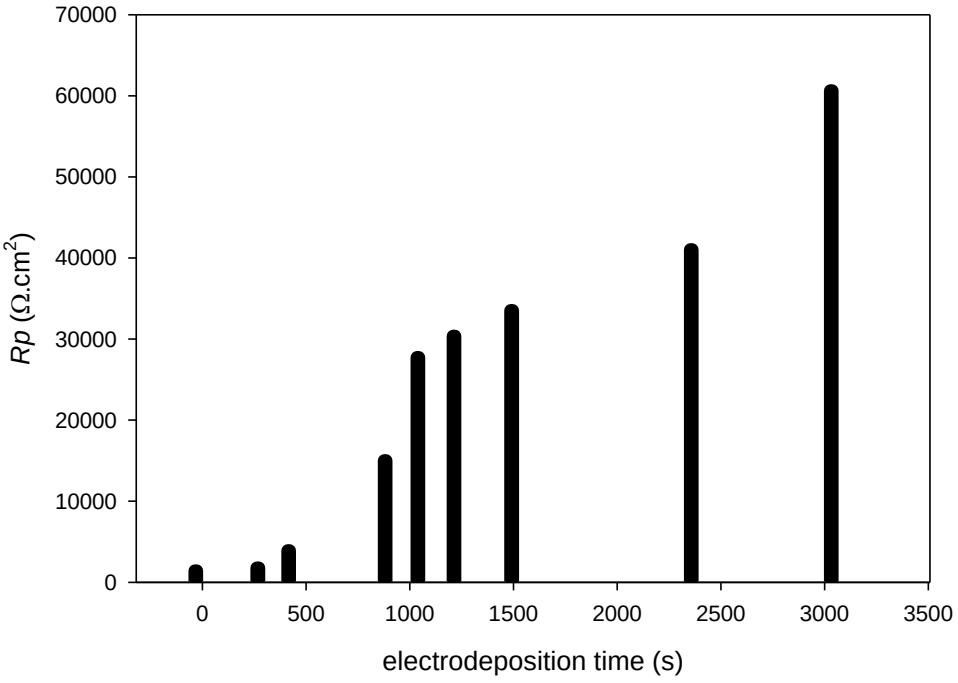

Fig. 7. Growth of polarization resistance during the electrodeposition process

4. Conclusions

On the basis of performed experiments, analysis of the results and their interpretations, we concluded the following conclusions:

- Calcium phosphate layer created by electrodeposition continuously covers the entire surface of the substrate and is formed by irregular branched units that overlap each other.
- Current density monitoring during calcium phosphate electrodeposition process is very important because of evaluation of correct processing. Curve with local maximum of current density followed by values towards to zero corresponds with good layer growth.
- Although after half an hour of the electrodeposition process there is no such significant decrease in current density, it is necessary to continue in the process in order to increase values of R_p and improve the corrosion resistance of created layer that way.
- Immediate polarization resistance of the surface with calcium phosphate layer after 5 minutes exposition in 0.9% NaCl is 43-times higher than polarization resistance of grinded surface.

Acknowledgements

The research is supported by European regional development fund and Slovak state budget by the project ITMS 26220220048 (call OPVaV-2008/2.2/01-SORO). Authors are grateful for the support of experimental works by project VEGA No. 1/0100/11

References

[1] H. Hamid, J. Coltart: Mcgill. J. Med. 10(2) (2007) 105–111.

[2] P. Peeters, M. Bosiers, J. Verbist, K. Deloose, B. Heublein: J. Endovasc. Ther. 12(1) (2005) 1–5.

[3] J. Heller, R. V. Sparer, G. Zentner: In: M. Chasin, R. S. Langer (eds.) Biodegradable Polymers as Drug Delivery Systems. M. Dekker, New York, 1990.

[4] O.M. Bostman: J. Bone Joint Surg. 73B(4) (1991) 679–682.

[5] J. Levesque, D. Dube, M. Fiset, D. Mantovani: Adv. Mater. Process. 162(9) (2004) 45–48.

[6] J. Vormann: Mol. Aspects Med. 24(1–3) (2003) 27–37.

[7] R. C. Zeng, W. Dietzel, F. Witte, N. Hort, C. Blawert: Adv. Eng. Mater. 10(8) (2008) 3–14.

[8] D. Upadhyay, A. P. Manoj, R. S. Dubey, V. K. Srivastava: Mater. Sci. Eng. A 432(1–2) (2006) 1–11.

[9] P. A. Dearnley: Surf. Coat. Technol. 198(1–3) (2005) 483–490.

[10] M. Jamesh, S. Kumar, T. S. N. Sankara Narayanan: J. Coat. Technol. Res. 9(4) (2011) 495-502.

[11] B. Mordike, T. Ebert: Mater Sci. Eng A 302(1) (2001) 37–45.

[12] H. Agins, N. Alcock, M. Bansal, E. Salvati, P. Wilson, P. Pellicci: J Bone Joint Surgery 70(3) (1988) 347-356.

[13] V. Langkamer, C. Case, P. Heap, A. Taylor, C. Collins, M. Pearse: J. Bone Joint Surgery 74(6) (1992) 831-838.

[14] T. Albrektsson: Crit. Rev. Biocomp. 1(1) (1985) 53–84.

[15] J. Black: J. Bone Joint Surgery 70(4) (1988) 517-519.

[16] R.M. Touyz: Front Biosci. 9 (2004) 1278–1293.

[17] B. Denkena, A. Lucas: CIRP Ann. – Manuf. Technol. 56(1) (2007) 113–116.

[18] B. Zberg, P.J. Uggowitzer, J.F. Löffler: Nat. Mater. 8(11) (2009) 887–891.

[19] F. Witte, V. Kaese, H. Haferkamp, E. Switzer, A. Meyer-Lindenberg, C.J. Wirth, H. Windhagen: Biomater. 26(17) (2005) 3557–3563.

[20] G. Song, A. Atrens: Adv. Eng. Mater. 5(12) (2003) 837–858.

[21] S. Shadanbaz, G. J. Dias: Acta Biomater. 8 (2012) 20–30.

[22] M. Osigo, Y. Yamashita, T. Matsumoto, J. Det. Res. 77 (1998) 1426-1434.

[23] L.P. Xu, G.N. Yu, E.L. Zhang, F. Pan, K. Yang, J. Biomed. Mater. Res. 83A(3) (2007) 703-711.

[24] Zhang Chun-Yan, Zeng Rong-Chang , Liu Cheng-Long , Gao Jia-Cheng: Surf. Coat. Technol. 204(21-22) (2010) 3636–3640.

[25] G. Song: Corr. Sci. 49 (2007) 1696-1701.

[26] Y. Song, D. Shan, R. Chen, F. Zhang, E. H. Han: Mater. Sci. Eng. C29(3) (2009) 1039-1045.

[27] T. Lothar: Labor und Diagnose, 5th edition, TH-Books, Frankfurt 2000.

[28] B. Hadzima, M. Bukovina, P. Doležal: Mater. Eng.-Mater. inž. 17(4) (2010) 14-19.

[29] Das, G. Liu, Z. Fan: Mater. Sci. Eng. A419(1-2) (2006) 349–356.

[30] N.T. Kirkland, M. P. Staiger, D. Nisbet, C.H.J. Davies, N. B. Birbilis: JOM 63(6) (2011) 28-34.

[31] ASM Handbook, Vol 9: Metallography and Microstructures. Ed: G.F. Van der Voort, ASM International, New York 2004.

[32] Y.W. Song, D.Y. Shan, E.H. Han: Mater. Letters 62(17-18) (2008) 3276-3279.